

Bubbles with attached quantum vortices in trapped binary Bose-Einstein condensates

Victor P. Ruban*

Landau Institute for Theoretical Physics, RAS, Chernogolovka, Moscow region, 142432 Russia

(Dated: August 30, 2021)

Specific topological excitations of energetically stable “core-and-mantle” configurations of trapped two-component immiscible Bose-Einstein condensates are studied numerically within the coupled Gross-Pitaevskii equations. Non-stationary long-lived coherent structures, that consist of several quantum vortex filaments penetrating the “mantle” from outside to inside and vice-versa and demonstrate quite nontrivial dynamics, are observed in simulations for the first time. The ends of filaments can remain attached to the interface between the “mantle” and the “core” if the latter is large enough while the surface tension is not small. The shapes of such “bubbles” are strongly affected by the vortices and sometimes are far from being spherical.

I. INTRODUCTION

Multi-component mixtures of ultracold Bose-Einstein-condensed atomic gases have been extensively studied over a quarter of century [1–5]. Such systems consist either of different chemical elements, or of different isotopes of the same element, or of the same isotope in different internal (hyperfine) quantum states. The interactions between different species give rise to a rich variety of unique features which do not exist for a single-component Bose-Einstein condensate (BEC). What is very important, parameters of nonlinear interactions for matter waves, being proportional to the scattering lengths, can be tuned in many cases via Feshbach resonances [6–10]. In particular, with a sufficiently strong cross-repulsion between two components, phase separation occurs [11, 12]. It lies in the base of many related configurations and phenomena of high interest, such as domain walls and surface tension between segregated condensates [4, 13], nontrivial ground state geometry of binary immiscible condensates in traps [14–16] (including optical lattices [17–19]), the dynamics of bubbles [20], the quantum counterparts of classical hydrodynamic instabilities (Kelvin-Helmholtz [21, 22], Rayleigh-Taylor [23–25], Plateau-Rayleigh [26], the parametric instability of capillary waves at the interface [27, 28]), complex textures in rotating binary condensates [29–31], vortices with filled cores [3, 32–37], three-dimensional topological structures [38–42], capillary flotation of dense drops in trapped immiscible BECs [43], etc.

Among other coherent structures, quantum vortices have long been recognized as objects of primary interest and importance. Already for single-component condensates, a lot of expressive results has been obtained on vortex configurations and their dynamics (see, e.g., [44–55], and references therein). Concerning vortices in mixed condensates, the realm is even larger and containing wide unknown territories. Many “godsend” are still possible there for an explorer. This work presents a new kind of rather elegant long-lived compound vortex-bubble

structures with nontrivial dynamics. To explain what they basically are, let us recall that in a two-component immiscible condensate, domain walls with attached quantum vortices are possible [41]. They are highly deformed vortex sheets of a special form. In Ref.[41], the authors investigated such complexes for the case of equal self-repulsion coefficients. Numerical solutions were obtained there for binary BECs in elongated traps where the equilibrium interface between the species was a disc with the edge at the Thomas-Fermi surface. Quantum vortices were present in both components and directed mainly along the trap axis.

Here it will be shown that essentially new and interesting feature arises when there is inequality (asymmetry) between the coefficients. In a nearly spherical harmonic trap, it results in formation of a stable and compact background equilibrium configuration of the “core-and-mantle” type. The presence of stably trapped, vortex-free “core” at the center, in combination with the surface tension between the components, tends to stabilize possible vortex filaments attached to such a bubble from outside and penetrating the “mantle” (see Fig.1 for example). Of course, the number of (outgoing) vortices is always equal to the number of (ingoing) antivortices. The density of the outer component is so negligible inside the “core” that practically it does not matter which of the vortices is the continuation of a given antivortex. Only the overall balance is usually essential. Each vortex or antivortex typically retains its identity and is directed roughly along the local radius. Due to interactions, the vortices are in transversal motion, simple or complicated. But sometimes, a pair of attached filaments (one ingoing and one outgoing) can dynamically couple, then get detached from the bubble and finally form a separate vortex filament. However, in such scenario the vortex pair has to overcome a “potential barrier” caused by surface tension. For relatively large bubbles and a small number of vortices, such processes occur quite rarely. Therefore structures of this kind are able to exist for thousands trap time units, as our numerical simulations show. We will also see that the dynamics becomes progressively more complicated with increasing number of attached vortices.

To the best of my knowledge, such three-dimensional complexes in trapped immiscible BECs have not yet been

*Electronic address: ruban@itp.ac.ru

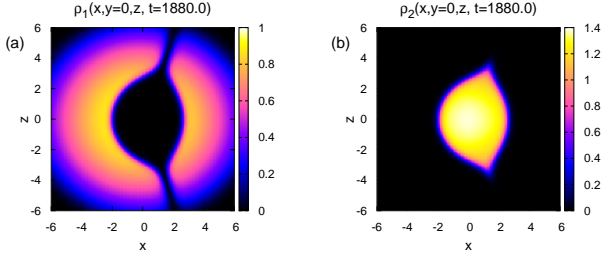


Figure 1: A numerical example of long-lived trapped condensate bubble with one pair of attached vortex filaments. Presented are normalized densities of the two condensate components in cross-section $y = 0$ (note the difference in the color scales): a) “mantle”; b) “core”. Transition layer between the clouds is rather sharp. The configuration is slowly rotating around z axis, with super-imposed oscillations of the interface, and it is shown at the moment when both vortices lie in plane $y = 0$. In this simulation $\lambda = 1.1$, $g_{11} = 1.0$, $g_{22} = 0.6$, $g_{12} = 1.2$, $n_1 = 1521.8$, $n_2 = 175.8$, and $\mu_1 = 30$.

discussed in the literature. Far-distant analogies are however known, as quantum vortices in crusts of neutron stars (see, e.g., review [56]), or ^3He - ^4He topological structures suggested in Ref.[57] (a droplet of ^4He immersed in the ^3He liquid). The purpose of this work is to introduce bubbles with attached quantum vortices theoretically in the context of ultracold gases and illustrate, on several representative numerical examples, their main properties. Scientific importance of these new structures is in their theoretical existence (and hopefully experimental feasibility) within wide and realistic parameter ranges, together with their quite nontrivial dynamics.

II. THE MODEL AND NUMERICAL METHOD

As the basic mathematical model in our research, we employ the widely recognized coupled Gross-Pitaevskii equations for two complex wave functions, $A(\mathbf{r}, t)$ (the first component, “mantle”), and $B(\mathbf{r}, t)$ (the second component, “core”). This conservative model is applicable for rarefied Bose-gases in the limit of zero temperature. For simplicity, equal masses $m_1 = m_2 = m$ of the species atoms are considered (or the small difference in mass of isotopes as, for example, ^{85}Rb and ^{87}Rb is neglected [8]). Let an axisymmetric harmonic trap be characterized by a perpendicular frequency ω_\perp and by an anisotropy $\lambda = \omega_\parallel/\omega_\perp$. With the trap units $\tau = 1/\omega_\perp$ for the time, $l_{\text{tr}} = \sqrt{\hbar/\omega_\perp m}$ for the length, and $\varepsilon = \hbar\omega_\perp$ for the energy, the equations of motion are written in dimensionless form

$$i\dot{A} = -\frac{1}{2}\nabla^2 A + [V(x, y, z) + g_{11}|A|^2 + g_{12}|B|^2] A, \quad (1)$$

$$i\dot{B} = -\frac{1}{2}\nabla^2 B + [V(x, y, z) + g_{21}|A|^2 + g_{22}|B|^2] B, \quad (2)$$

where $V = (x^2 + y^2 + \lambda^2 z^2)/2$ is the trap potential, and $g_{\alpha\beta}$ is the symmetric 2×2 matrix of nonlinear interactions. Physically, the interactions are determined by the scattering lengths $a_{\alpha\beta}$ [2]:

$$g_{\alpha\beta}^{\text{phys}} = 2\pi\hbar^2 a_{\alpha\beta} (m_\alpha^{-1} + m_\beta^{-1}). \quad (3)$$

We are interested in the case of all positive $g_{\alpha\beta}$. Without loss of generality, the first self-repulsion coefficient can be normalized to the unit value, $g_{11} = 1$, since we consider $g_{\alpha\beta}$ as constant in time parameters throughout this work. With this choice, the (conserved) numbers of trapped atoms are given by relations

$$N_1 = \frac{l_{\text{tr}}}{4\pi a_{11}} \int |A|^2 d^3\mathbf{r} = (l_{\text{tr}}/a_{11})n_1, \quad (4)$$

$$N_2 = \frac{l_{\text{tr}}}{4\pi a_{11}} \int |B|^2 d^3\mathbf{r} = (l_{\text{tr}}/a_{11})n_2. \quad (5)$$

In real experiments the ratio l_{tr}/a_{11} ranges typically from a few hundreds to a few thousands.

It is a well known fact that system (1)-(2) in the phase-separated regime is similar to potential flows in the classical hydrodynamics of two immiscible compressible fluids, except for the vicinity of domain walls and vortex cores where the “quantum pressures” come into play. The “hydrodynamic pressures” of the first and the second matter-wave “fluids” are $g_{11}|A|^4/2$ and $g_{22}|B|^4/2$ respectively, and across the interface they are approximately equal (the difference caused by surface tension and by slow flows is relatively small). At equal pressures, the component with smaller self-repulsion coefficient is more dense. Therefore, in order to ensure a relatively dense and stable core, it is necessary to satisfy the inequality $g_{22} < g_{11} = 1$.

It is a known fact that equilibrium states are characterized by two chemical potentials μ_1 and μ_2 . Under relevant conditions $\mu_1 \gg 1$ and $\mu_2 \gg 1$, the background density profiles are given by the Thomas-Fermi approximation:

$$|A_0|^2 \approx [\mu_1 - V(x, y, z)] \equiv \mu_1 \rho_{1\text{eq}}(\mathbf{r}), \quad (6)$$

$$|B_0|^2 \approx [\mu_2 - V(x, y, z)]/g_{22} \equiv \mu_1 \rho_{2\text{eq}}(\mathbf{r}), \quad (7)$$

where we have introduced the normalized densities $\rho_1 = |A|^2/\mu_1$ and $\rho_2 = |B|^2/\mu_1$. The first formula is valid in the mantle, while the second one in the core. An effective transverse size of the condensate is thus $R_\perp = \sqrt{2\mu_1}$, while a characteristic width of vortex lines in the mantle is $\xi \sim 1/\sqrt{\mu_1}$.

The following condition for phase separation is assumed [11, 12],

$$g = (g_{12}^2 - g_{11}g_{22}) > 0.$$

There is a narrow transition layer between the segregated condensates (its width is roughly proportional to $1/\sqrt{g}$; it is also seen in Fig.1) and the associated surface tension

roughly proportional to \sqrt{g} [11, 13]. Numerical simulations performed here were oriented on experimentally realizable ^{85}Rb - ^{87}Rb mixtures [8], where $a_{12}/a_{22} \approx 2$ while a_{11} can be tuned via Feshbach resonance. Therefore in all our runs $g_{12} = 2g_{22}$. On the other hand, an optimal value for the ratio g_{22}/g_{11} should simultaneously provide a large surface tension, and be not close to unity for core stability. We typically put $g_{22} = 0.5$ or 0.6 in this work, but in some runs, for comparison, $g_{22} = 0.3$ or 0.8 .

The coupled Gross-Pitaevskii equations (1)-(2) were simulated using a standard Split-Step Fourier Method of the second order accuracy. Spatial and temporal resolutions were sufficient to conserve the corresponding Hamiltonian functional and the numbers of particles n_1 and n_2 up to the 5th decimal place over time period $T_{\text{run}} = 2000$.

Initial states containing only soft excitations were prepared by application of the gradient descent procedure, which in the given case is equivalent to an imaginary-time propagation for a finite period of an auxiliary time-like variable. The input for this dissipative procedure was a configuration of the first component as $A_{\text{inp}} = \tilde{A}_0(\mathbf{r})C_0(\mathbf{r})$, with a real $\tilde{A}_0(\mathbf{r})$. Several vortex filaments were introduced through the complex multiplier

$$C_0(\mathbf{r}) = \prod_j \frac{w_j}{\sqrt{|w_j|^2 + \epsilon}}, \quad (8)$$

where explicit form for $w_j(\mathbf{r})$ depended upon the desired input vortex shape. In particular, a filament oriented roughly in z direction was introduced by

$$w_j = [x - X_j(z)] \pm i[y - Y_j(z)], \quad (9)$$

with relatively small arbitrary functions $X_j(z)$ and $Y_j(z)$. Accordingly, x or y variable parameterized vortex filaments oriented closely to x or y direction, respectively. A small positive ϵ was employed to avoid zero in the denominators. The choice \pm imposed the sign of rotation of the j -th vortex. In the output, every such filament gave one vortex and one antivortex in the above discussed sense. The “seed” $B_{\text{inp}} = \tilde{B}_0(\mathbf{r})$ for the second component contained no vortices.

The dissipative procedure “filtered out” fast potential excitations and brought the system density closely to its background equilibrium configuration Eqs.(6-7), including the specific narrow wall profile between the mantle and the core. Correct cross-sections of the vortices were formed as well, adjusted to the background density. At the same time, slow excitations as vortex positions could not achieve a minimum of their energy during a relatively short imaginary-time propagation, and this fact resulted in subsequent nontrivial vortex dynamics at the main, conservative stage of simulation. Taking different values for μ_1 and μ_2 , various vortex configurations $X_j(z)$ and $Y_j(z)$ as the input of the dissipative procedure, and different periods for the imaginary-time propagation, it was possible to achieve different values of n_1 , n_2 , as well as various initial arrangements of the attached vortices.

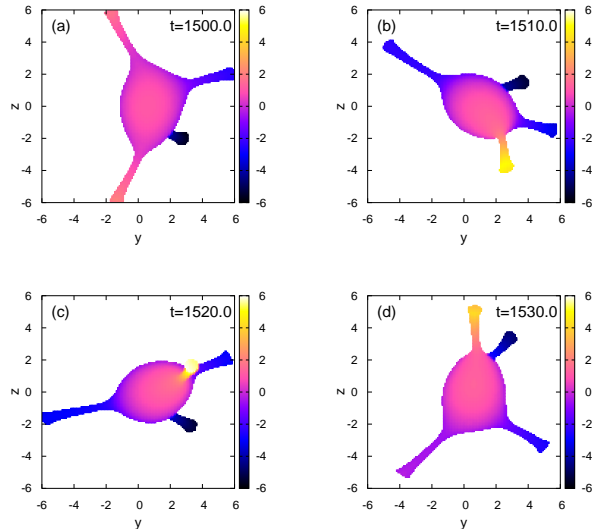


Figure 2: A long-lived nonstationary bubble with two pairs of attached vortices. The color scale corresponds to x -coordinate of the grid points nearest to the surface determined by equation $\rho_1(\mathbf{r}, t) = 0.5\rho_{1\text{eq}}(\mathbf{r})$. Only points within the domain $\rho_{1\text{eq}}(\mathbf{r}) > 0.2$ are shown, and therefore the outer ends of filaments are truncated. In this simulation the structure is not simply rotating around a time-dependent instant axis (not aligned with z -axis), but also is subjected to slow deformations. In general, it resembles somersaults. The parameters are: $\lambda = 1.1$, $g_{11} = 1.0$, $g_{22} = 0.6$, $g_{12} = 1.2$, $n_1 = 1552.2$, $n_2 = 117.9$, and $\mu_1 = 30$.

The trap anisotropy was chosen not far from unity, typically $\lambda = 1.1$. That was done in order to break the spherical symmetry, but just slightly.

It should be said that no short-scale instabilities were observed in our simulations. The structures never decay if a small perturbation is present. This fact can be viewed as an indirect evidence of their dynamical stability. Some of the obtained numerical results are presented and discussed in the next section.

III. RESULTS

The simplest case of trapped bubble with just one pair of attached vortex filaments is presented in Fig.1. It is clearly seen there that the “kernel” is far from being spherical, since the vortex ends pull the interface. In particular, the kernel boundary has sharp conical features near the vortex ends. In this example, the initial vortex configuration was nearly symmetric with respect to the equatorial plane $z = 0$, so the motion is a simple slow rotation around z -axis accompanied by bubble oscillations due to “imperfect” initial conditions (see video [58]). In another run, without equatorial symmetry, the motion was slightly less monotonous, because an instant axis of rotation depended on time (not shown).

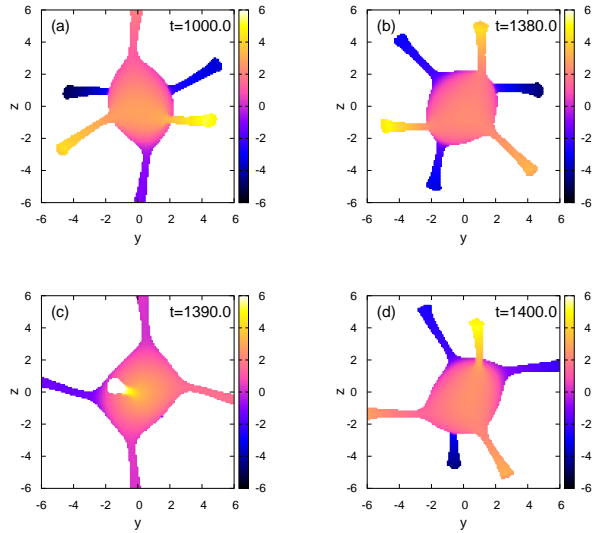


Figure 3: A regularly rotating bubble with three pairs of attached vortices. The parameters are: $\lambda = 1.1$, $g_{11} = 1.0$, $g_{22} = 0.8$, $g_{12} = 1.6$, $n_1 = 1503.3$, $n_2 = 141.7$, and $\mu_1 = 30$. Initially, the vortices were oriented roughly along the three Cartesian axes. The instant rotational axis is slowly precessing around z -direction.

The behavior becomes nontrivial starting from two pairs of attached vortices. An example is shown in Fig.2 where the shape of an effective (inner) boundary of the first component is presented for several time moments. In this case, the motion resembles some gymnastic performance, with somersaults, or a skydiver tumbling through the air (see video [59]). Of course, more “tranquil” regimes are also possible, when a nearly stationary configuration is rotating around z -axis, similarly to the previous example.

Three and more pairs of attached vortices have been observed to demonstrate, depending on parameters and initial conditions, both a regular and a highly dramatic and unstable dynamics. The regular dynamics corresponds to the simplest case when a symmetric bundle of several vortices is in a nearly stationary rotation around z -axis, and also to a slightly more nontrivial case when the rotation is around a precessing instant axis (see Fig.3 and video [60] as an example). Such quiet regimes are more typical for larger surface tension, for example with $g_{22} = 0.8$. Contrary to that, with $g_{22} = 0.5, 0.6$ the bubble-vortex complexes often behave irregularly, so the mutual arrangement of vortices evolves in a complicated and seemingly unpredictable manner. Using again comparison with athletic exercises, we may say that such a performance could be only possible for a fantastic, perfectly supple clown possessing more than two pairs of legs/arms. Indeed the movements look sometimes rather funny (see video [61]). An example of a sequence of changes for a bubble with three pairs of attached fila-

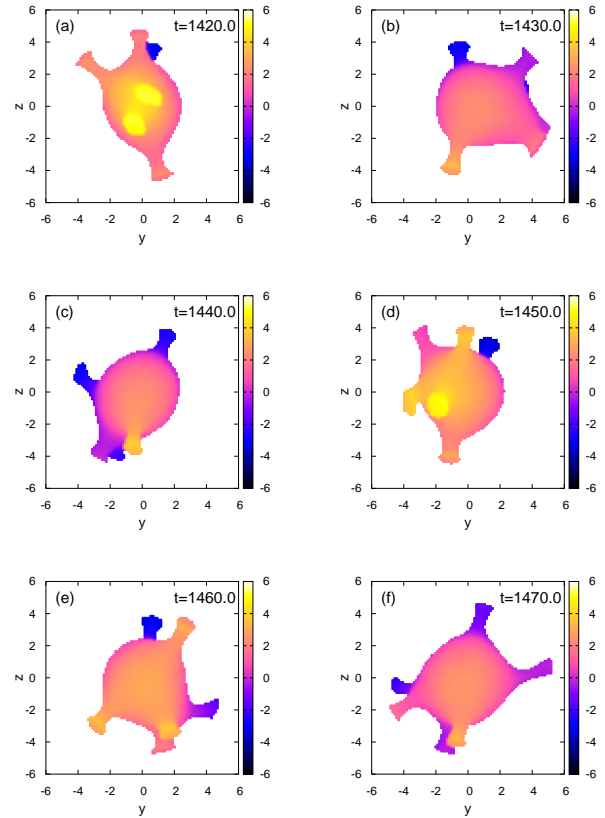


Figure 4: A nonstationary bubble with three pairs of attached vortices. The parameters are: $\lambda = 1.1$, $g_{11} = 1.0$, $g_{22} = 0.5$, $g_{12} = 1.0$, $n_1 = 332.5$, $n_2 = 145.7$, and $\mu_1 = 18$. In this example the dynamics of vortices is rather fast and dramatic, while the numbers of particles are relatively small.

ments is presented in Fig.4 (extracted from video [61]). This numerical experiment also demonstrates that required numbers of trapped atoms may be relatively small for possibility of the phenomenon under consideration. So, with a realistic trap length ($l_{tr}/a_{11}) \approx 100$, we have $N_1 \approx 3.3 \times 10^4$ and $N_2 \approx 1.5 \times 10^4$.

It should be said again that during unstable dynamics, the ends of two vortices with opposite signs often approach one another and in some cases they can connect and break away from the bubble, thus forming a separate filament (two examples are seen in videos [61, 62]). Very easy it occurs in the case of weak surface tension (in particular, when $g_{22} = 0.3$). If surface tension is sufficiently strong, such behavior is typical mainly for systems with relatively small cores. The vortex filaments in the mantle are then rather energetic and in fully three-dimensional regime, so that they have opportunity to be tilted at large angles to the local bubble normal, thus initiating the process of separation.

Contrary to that, a relatively large heavy core and thin mantle make the vortices short (while the flows of the first component approximately two-dimensional

along the spheroid) and directed strictly perpendicular, and their dynamics is then qualitatively similar to motion of point vortices on a spheroidal surface. However, the question of quantitative applicability of that analogy requires further thorough investigation, because interactions of vortices with potential oscillations of the mantle may still remain important. In general, this situation resembles the vortex-antivortex physics in shell-shaped ordinary BECs [55]. Fig.4 corresponds to an intermediate regime between fully three-dimensional and effectively two-dimensional regimes.

From all the above examples it has been clear that the dynamics of attached vortices can be approximately finite-dimensional, in the sense that a finite number of soft degrees of freedom is effectively involved. Apparently, the motion of attached vortices strongly depends on their initial arrangement. Numerically, it is easy to prepare a practically arbitrary initial state. However, it should be stressed here that our numerical initialization procedure has nothing to do with a required real experimental procedure to produce bubbles with attached vortices. But at this point we may recall that “rotating” trap potentials

$$V(\mathbf{r}, t) = (x^2 + y^2 + \lambda^2 z^2)/2 + \nu(t)\text{Re}[(x + iy)^2 e^{-2i\phi(t)}]$$

are known to “pull” vortex filaments from the periphery towards the condensate axis. Here $\phi(t)$ is the rotation angle, while $\nu(t)$ is an anisotropy parameter in (x, y) plane. Suppose we initially have a nearly equilibrium state with a short vortex filament located near the outer boundary of the mantle. As the trap begins rotate, the filament approaches the core, gets attached to it and then forms a vortex-antivortex pair. The core remains vortex-free in this process. At least several numerical simulations (not illustrated here) have demonstrated the validity of such scenario for configurations similar to that shown in Fig.1, including the asymmetry around z axis. Angular velocity of the trap is an important parameter in such situations. If we make the rotation faster, then two, three or a larger number of vortex pairs can be attached to the bubble as the result of a complicated and essentially non-equilibrium transient process, with each vortex being oriented at some not very large angle to z axis (see an example in Fig.5). Thus, rotating trap seems as one of the possible experimental ways. As to the more general problem how to produce in the laboratory a bubble with several arbitrary arranged attached vortices, it requires a separate and deep investigation including efforts of highly qualified experimentalists. Therefore it is beyond the present purely theoretical consideration.

IV. CONCLUSIONS

To summarize, specific wall-vortex complexes in a two-component BEC, in combination with its compact, stably stratified trapped configuration, have been theoretically introduced in this work. These are long-lived bubbles with attached vortices existing in wide parametric ranges and demonstrating quite interesting dynamical behavior in the numerical experiments. Both regular and irregular regimes have been observed. Since we have here a new example of rich physics contained in a relatively simple (at least for numerical investigation) structure, further theoretical efforts in this direction are necessary, including development of an analytical approach.

The parameters of our simulations are quite realistic, so future experimental implementation of such systems seems possible. A challenge for experimentalists will be perhaps to produce a binary condensate without small droplets and multiple domains, but with just a single core at the center, and after that to imprint several vortices into the shell. Rotating trap is a possible technique.

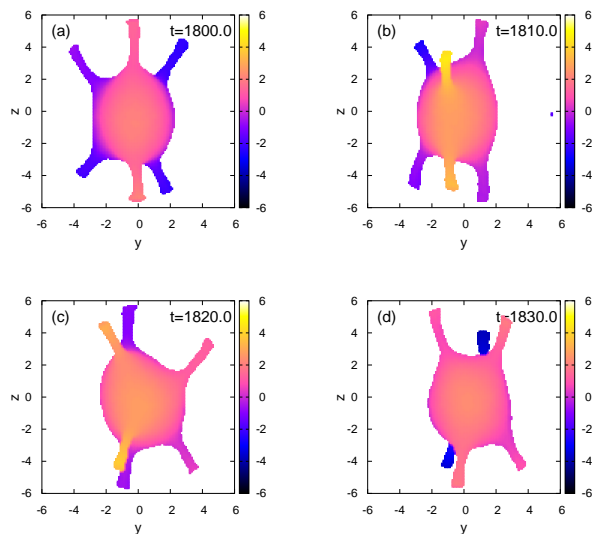


Figure 5: A bubble with three pairs of attached vortices produced by rotating trap with the rotation angle $\phi(t) = 0.08 \cdot 2\pi(\sqrt{t^2 + 400^2} - 400)$, and the transversal anisotropy $\nu(t) = 0.05t^2/(t^2 + 400^2)$. The remaining parameters are: $\lambda = 1.0$, $g_{11} = 1.0$, $g_{22} = 0.6$, $g_{12} = 1.2$, $n_1 = 894.7$, $n_2 = 182.5$, and $\mu_1 = 24$. In this figure, the outer ends of vortices are truncated by the condition $\rho_{1eq}(\mathbf{r}) > 0.3$.

-
- [1] Tin-Lun Ho and V. B. Shenoy, Phys. Rev. Lett. **77**, 3276 (1996).
 - [2] H. Pu and N. P. Bigelow, Phys. Rev. Lett. **80**, 1130 (1998).

- [3] B. P. Anderson, P. C. Haljan, C. E. Wieman, and E. A. Cornell, Phys. Rev. Lett. **85**, 2857 (2000).
- [4] S. Coen and M. Haelterman, Phys. Rev. Lett. **87**, 140401 (2001).

- [5] G. Modugno, M. Modugno, F. Riboli, G. Roati, and M. Inguscio, Phys. Rev. Lett. **89**, 190404 (2002).
- [6] J. P. Burke, Jr., J. L. Bohn, B. D. Esry, and C. H. Greene, Phys. Rev. Lett. **80**, 2097 (1998).
- [7] G. Thalhammer, G. Barontini, L. De Sarlo, J. Catani, F. Minardi, and M. Inguscio, Phys. Rev. Lett. **100**, 210402 (2008).
- [8] S. B. Papp, J. M. Pino, and C. E. Wieman, Phys. Rev. Lett. **101**, 040402 (2008).
- [9] S. Tojo, Y. Taguchi, Y. Masuyama, T. Hayashi, H. Saito, and T. Hirano, Phys. Rev. A **82**, 033609 (2010).
- [10] C. Chin, R. Grimm, P. Julienne, and E. Tiesinga, Rev. Mod. Phys. **82**, 1225 (2010).
- [11] E. Timmermans, Phys. Rev. Lett. **81**, 5718 (1998).
- [12] P. Ao and S. T. Chui, Phys. Rev. A **58**, 4836 (1998).
- [13] B. Van Schaeybroeck, Phys. Rev. A **78**, 023624 (2008).
- [14] A. A. Svidzinsky and S. T. Chui, Phys. Rev. A **68**, 013612 (2003).
- [15] S. Gautam and D. Angom, J. Phys. B: At. Mol. Opt. Phys. **43**, 095302 (2010).
- [16] R. W. Pattinson, T. P. Billam, S. A. Gardiner, D. J. McCarron, H. W. Cho, S. L. Cornish, N. G. Parker, and N. P. Proukakis, Phys. Rev. A **87**, 013625 (2013).
- [17] K. Suthar, Arko Roy, and D. Angom, Phys. Rev. A **91**, 043615 (2015).
- [18] K. Suthar and D. Angom, Phys. Rev. A **93**, 063608 (2016).
- [19] K. Suthar and D. Angom, Phys. Rev. A **95**, 043602 (2017).
- [20] K. Sasaki, N. Suzuki, and H. Saito, Phys. Rev. A **83**, 033602 (2011).
- [21] H. Takeuchi, N. Suzuki, K. Kasamatsu, H. Saito, and M. Tsubota, Phys. Rev. B **81**, 094517 (2010).
- [22] N. Suzuki, H. Takeuchi, K. Kasamatsu, M. Tsubota, and H. Saito, Phys. Rev. A **82**, 063604 (2010).
- [23] K. Sasaki, N. Suzuki, D. Akamatsu, and H. Saito, Phys. Rev. A **80**, 063611 (2009).
- [24] S. Gautam and D. Angom, Phys. Rev. A **81**, 053616 (2010).
- [25] T. Kadokura, T. Aioi, K. Sasaki, T. Kishimoto, and H. Saito, Phys. Rev. A **85**, 013602 (2012).
- [26] K. Sasaki, N. Suzuki, and H. Saito, Phys. Rev. A **83**, 053606 (2011).
- [27] D. Kobayakov, V. Bychkov, E. Lundh, A. Bezett, and M. Marklund, Phys. Rev. A **86**, 023614 (2012).
- [28] D. K. Maity, K. Mukherjee, S. I. Mistakidis, S. Das, P. G. Kevrekidis, S. Majumder, and P. Schmelcher, Phys. Rev. A **102**, 033320, (2020).
- [29] K. Kasamatsu, M. Tsubota, and M. Ueda, Phys. Rev. Lett. **91**, 150406 (2003).
- [30] K. Kasamatsu and M. Tsubota, Phys. Rev. A **79**, 023606 (2009).
- [31] P. Mason and A. Aftalion, Phys. Rev. A **84**, 033611 (2011).
- [32] K. J. H. Law, P. G. Kevrekidis, and L. S. Tuckerman, Phys. Rev. Lett. **105**, 160405 (2010).
- [33] M. Pola, J. Stockhofe, P. Schmelcher, and P. G. Kevrekidis, Phys. Rev. A **86**, 053601 (2012).
- [34] S. Hayashi, M. Tsubota, and H. Takeuchi, Phys. Rev. A **87**, 063628 (2013).
- [35] A. Richaud, V. Penna, R. Mayol, and M. Guilleumas, Phys. Rev. A **101**, 013630 (2020).
- [36] A. Richaud, V. Penna, and A. L. Fetter, Phys. Rev. A **103**, 023311 (2021).
- [37] V. P. Ruban, JETP Lett. **113**, 532 (2021).
- [38] K. Kasamatsu, M. Tsubota, and M. Ueda, Phys. Rev. Lett. **93**, 250406 (2004).
- [39] H. Takeuchi, K. Kasamatsu, M. Tsubota, and M. Nitta, Phys. Rev. Lett. **109**, 245301 (2012).
- [40] M. Nitta, K. Kasamatsu, M. Tsubota, and H. Takeuchi, Phys. Rev. A **85**, 053639 (2012).
- [41] K. Kasamatsu, H. Takeuchi, M. Tsubota, and M. Nitta, Phys. Rev. A **88**, 013620 (2013).
- [42] S. B. Gudnason and M. Nitta, Phys. Rev. D **98**, 125002 (2018).
- [43] V. P. Ruban, JETP Lett. **113**, 814 (2021).
- [44] C. J. Pethick and H. Smith, *Bose-Einstein Condensation in Dilute Gases*, (Cambridge University Press, Cambridge, 2002).
- [45] L. P. Pitaevskii and S. Stringari, *Bose-Einstein Condensation* (Oxford University Press, Oxford, 2003).
- [46] A. L. Fetter, Rev. Mod. Phys. **81**, 647 (2009).
- [47] A. A. Svidzinsky and A. L. Fetter, Phys. Rev. A **62**, 063617 (2000).
- [48] V. P. Ruban, Phys. Rev. E **64**, 036305 (2001).
- [49] A. Aftalion and I. Danaila, Phys. Rev. A **68**, 023603 (2003).
- [50] T.-L. Horng, S.-C. Gou, and T.-C. Lin, Phys. Rev. A **74**, 041603(R) (2006).
- [51] S. Serafini, L. Galantucci, E. Iseni, T. Benaïme, R. N. Bisset, C. F. Barenghi, F. Dalfó, G. Lamporesi, and G. Ferrari, Phys. Rev. X **7**, 021031 (2017).
- [52] C. Ticknor, W. Wang, and P. G. Kevrekidis, Phys. Rev. A **98**, 033609 (2018).
- [53] V. P. Ruban, JETP Lett. **108**, 605 (2018).
- [54] C. Ticknor, V. P. Ruban, and P. G. Kevrekidis, Phys. Rev. A **99**, 063604 (2019).
- [55] K. Padavić, K. Sun, C. Lannert, and S. Vishveshwara, Phys. Rev. A **102**, 043305 (2020).
- [56] N. Chamel and P. Haensel, Liv. Rev. Relat. **11**, 10 (2008).
- [57] G. E. Volovik, Proc. Natl. Ac. Sci. USA **97**, 2431 (2000).
- [58] <http://home.itp.ac.ru/~ruban/12APR2021/v1.avi>
- [59] <http://home.itp.ac.ru/~ruban/12APR2021/v2.avi>
- [60] <http://home.itp.ac.ru/~ruban/12APR2021/v3.avi>
- [61] <http://home.itp.ac.ru/~ruban/12APR2021/v4.avi>
- [62] <http://home.itp.ac.ru/~ruban/12APR2021/v5.avi>